Force production by single kinesin motors

Mark J. Schnitzer*†, Koen Visscher‡†§ and Steven M. Block¶

*Biological Computation Research Department, Bell Laboratories, Lucent Technologies, Murray Hill, New Jersey 07974, USA
‡Departments of Physics and Molecular and Cellular Biology, University of Arizona, Tucson, Arizona 85721, USA
¶Departments of Applied Physics and Biological Sciences, Stanford University, Stanford, California 94305, USA
†These authors contributed equally to this work.
§e-mail: visscher@physics.arizona.edu

Motor proteins such as kinesin, myosin and polymerase convert chemical energy into work through a cycle that involves nucleotide hydrolysis. Kinetic rates in the cycle that depend upon load identify transitions at which structural changes, such as power strokes or diffusive motions, are likely to occur. Here we show, by modelling data obtained with a molecular force clamp, that kinesin mechanochemistry can be characterized by a mechanism in which a load-dependent isomerization follows ATP binding. This model quantitatively accounts for velocity data over a wide range of loads and ATP levels, and indicates that movement may be accomplished through two sequential 4-nm substeps. Similar considerations account for kinesin processivity, which is found to obey a load-dependent Michaelis–Menten relationship.

The mechanoenzyme kinesin has two motor domains[1] and travels processively along microtubules in discrete steps of 8 nm (ref. 2). The velocity of single kinesin motors moving along microtubules, v, has an ATP dependence that obeys Michaelis–Menten kinetics. This is the case over a broad range of loads, from near zero[3,4] to at least 5.5 pN, which represents a significant fraction of the kinesin stall force[5–9]. Moreover, the mechanochemical coupling ratio — defined as the number of ATP molecules hydrolysed per mechanical step — remains 1:1 over a similar range of loads[5]. Most theoretical models of kinesin movement invoke forms of loose coupling[10–13]; these predict that the apparent Michaelis–Menten constant for movement, K_M, should either remain constant or fall as the load increases and the ATP coupling ratio declines[6,12,14]. Experimentally, however, K_M has been found to increase with increasing load, implying that load affects the kinesin cycle in two distinct ways, lowering not only the turnover rate, but also the rate at which ATP molecules bind and commit to the reaction pathway[5]. This behaviour is inconsistent with most loosely-coupled theoretical models in their current forms. Here we explore the consequences of a tightly-coupled model that explicitly incorporates the two effects of load on Michaelis–Menten kinetics.

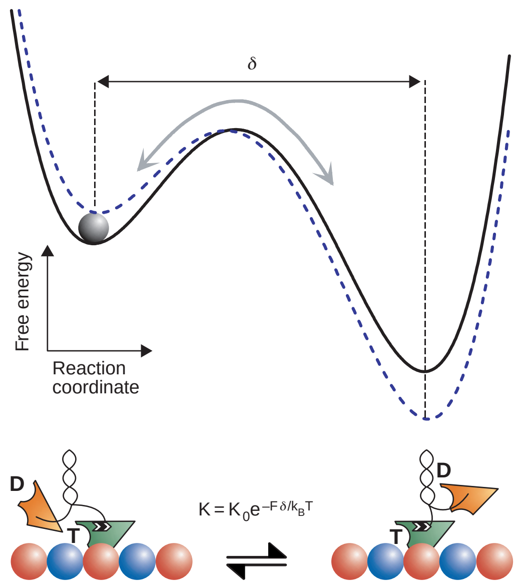

Figure 1 **Load-dependent isomerization.** Top, schematic free-energy diagram, showing a single barrier between two potential wells separated by a distance δ, before (dashed line) and after (solid line) application of external load. Here, each well represents a substate in a conformationally composite state and the reaction coordinate corresponds to the component of displacement along the long axis of the microtubule. A kinesin molecule undergoes rapid fluctuations between the two conformational substates, corresponding to back-and-forth transitions between potential minima. Bottom, diagrammatic representation of such a conformational composite, corresponding to fluctuations of the unbound kinesin head (orange); the partner head (green) remains tightly bound to the microtubule (red, blue). The equilibrium constant for this transition, K, is load-dependent; k_BT is the thermal energy.

Results

The energy-landscape model. For a motor with steps of size d, we use:

$$v(F, [\mathrm{ATP}]) = \frac{V_{max}[\mathrm{ATP}]}{[\mathrm{ATP}]+K_M} = \frac{d{\cdot}k_{cat}(F)[\mathrm{ATP}]}{[\mathrm{ATP}]+k_{cat}(F)/k_b(F)} \qquad (1)$$

where $V_{max} = d \cdot k_{cat}$ is the velocity at saturating levels of ATP, k_{cat} is the catalytic-turnover rate constant, and k_b is the apparent second-order rate constant for ATP binding, equal to the ratio k_{cat}/K_M. Both load-dependent rate constants, k_{cat} and k_b, decline with increased external load on the motor, F. Equation (1) implies tight coupling with a 1:1 ratio (if the coupling ratio were fixed but not equal to one, its value would simply multiply the numerator). The increase in K_M with load implies that the function $k_b(F)$ must decline faster with load than the function $k_{cat}(F)$ (ref. 5). To express these functions, we reasoned by analogy with recent work[15] on RNA polymerase (RNAP).

The RNAP transcription cycle can be modelled as a sequence of load-independent biochemical transitions together with a single, load-dependent mechanical transition occurring over a free energy barrier. The time required for a mechanical transition over this barrier rises exponentially with load, so the net rate of transcription follows a Boltzmann-type relationship[15,16]:

$$k(F) = \frac{k_0}{p + qe^{F\delta/k_BT}} \quad (2)$$

where k_0 is the unloaded rate constant, k_BT is the thermal energy, δ represents the characteristic distance over which the load acts, and p and $q = (1 - p)$ are the fractions of the unloaded catalytic cycle required for biochemical and mechanical transitions, respectively[15]. However, this description is incomplete for kinesin, because it omits the effects of load on k_b. These are incorporated as follows:

In a generalized kinesin ATPase pathway with N intermediate states,

$$1 \underset{k_{-1}}{\overset{k_1[\mathrm{ATP}]}{\longleftrightarrow}} 2 \underset{k_{-2}}{\overset{k_2}{\longleftrightarrow}} 3 \cdots \underset{k_{-(N-1)}}{\overset{k_{N-1}}{\longleftrightarrow}} N \underset{k_{-N}}{\overset{k_N}{\longleftrightarrow}} 1 \quad (3)$$

load has two effects. It lowers ATP affinity, by reducing k_1 and/or by increasing k_{-1}. It also reduces the turnover rate, by reducing the rate constant for (at least) one transition downstream of ATP binding. Together, these two effects produce the observed rise in K_M and the drop in k_b with load[5]. In the energy-landscape formalism, $k_{cat}(F)$ and $k_b(F)$ each have both biochemical and mechanical components, and therefore take the form of equation (2):

$$k_{cat}(F) = \frac{k^0_{cat}}{p_{cat} + q_{cat}e^{F\delta_{cat}/k_BT}}, \quad k_b(F) = \frac{k^0_b}{p_b + q_b e^{F\delta_b/k_BT}} \quad (4)$$

As explored recently for RNAP[15], there are several candidate mechanisms that generate relations of this form — these include an irreversible mechanical transition, a load-dependent inactivation that branches off the main catalytic cycle, or a load-dependent conformationally-composite state. For the kinesin system, the composite-state model is the most appropriate, as ATP binding is known to be highly reversible and there is currently no evidence for an inactive state off the main cycle. The composite-state model also represents the simplest possibility, because the two effects of load on catalysis and binding can be produced by a single composite state occurring immediately after ATP binding, at state 2 (equation (3)). State 2 is almost unique in this regard, because it adjoins the binding and catalysis phases of the cycle: transition rate constants leading out of this state may therefore strongly affect both k_{cat} and k_b. A load-dependent composite state occurring later in the cycle would have little influence on k_b, unless two or more reverse reactions were rapid, which does not seem to be the case for the kinesin cycle[17–21]. Thus, we restrict our attention to a model in which the composite state occurs at state 2.

In such a composite state, there are two conformational substates in near-equilibrium, separated by a free-energy barrier (Fig. 1). This is commonly referred to as a rapid isomerization in the actomyosin literature[22]. Load slows the velocity by shifting the equilibrium towards the rearward substate. This lowers the rate constant, k_2, for proceeding onwards in the cycle from the forward conformation, thereby lowering k_{cat}. It also increases the reverse rate constant, k_{-1}, leading to increased unbinding of ATP from the rearward conformation and thereby reducing ATP affinity. In this model, $\delta_{cat} = \delta_b$ refers to the identical conformational change, hereafter denoted by δ. Thus, if K_0 is the equilibrium constant between the two isomerization substates in the absence of load, then the load dependencies of k_2 and k_{-1} are given by:

$$k_2(F) = \frac{k'_2 K_0}{K_0 + e^{F\delta/k_BT}}, \quad k_{-1}(F) = \frac{k'_{-1}e^{F\delta/k_BT}}{K_0 + e^{F\delta/k_BT}} \quad (5)$$

In equation (5), k'_2 is the rate constant for the transition from the forward substate to state 3, and k'_{-1} is the rate constant for the transition from the rearmost substrate to state 1. Load alters the relative probabilities of these two substates, thereby affecting k_{cat} and k_b through their dependence on k_2 and k_{-1} (equation (5)), but it does not alter the value of k'_2 or k'_{-1}. At zero load ($F = 0$), $k_2 = k'_2K_0/(K_0 + 1)$ and $k_{-1} = k'_1/(K_0 + 1)$, because the unloaded-occupation probabilities of the forward and rearward substates are $K_0/(K_0 + 1)$ and $1/(K_0 + 1)$, respectively. Although δ is the same for k_{cat} and k_b (equation (4)), the various other rate constants in the ATPase cycle (equation (3)), such as k_3 and k_{-4}, enter the mathematical expressions for k_b and k_{cat} differently. Thus, the four other model parameters in equation (4) (k^0_b, k^0_{cat}, p_{cat}, and p_b) are independent and are not expected to be equal for binding and catalysis. In principle, load might act at additional points on the kinesin pathway, but the simple composite-state mechanism is attractive because it reconciles existing biochemical[17–21,23,24], structural[25] and mechanical[3,5,26] data. Other possible effects of load may be weaker, or may affect transitions that are not rate-limiting.

Predictions and fits of the kinesin model. The composite-state model makes several key predictions. First, kinesin motility should remain tightly coupled to ATP hydrolysis even under load, because conformational changes occur before hydrolysis. This prediction seems to be borne out, because the coupling ratio remains at 1 ATP per 8-nm step at near zero load[3,26] and under loads of up to ~5 pN (ref. 5).

Second, the model predicts that the kinesin–microtubule complex undergoes a significant conformational change upon binding of ATP. Just such a change has recently been reported for single-headed kinesin constructs[25], corresponding to a disorder-to-order transition in the neck linker region. In brief, the kinesin neck linker, a domain important for both motility and directionality[27–30], was found to exist in a mobile equilibrium between at least two conformations when bound to ADP[25]. Neck mobility ceases and the linker subdomain becomes tightly associated with the kinesin catalytic core when the head binds to ATP or to non-hydrolysable ATP analogues[25]. In contrast, binding to ADP or loss of the nucleotide frees the linker to enter the mobile, disordered state. Furthermore, biochemical studies of double-headed kinesin in solution have shown that ATP binding by one of the two kinesin heads triggers ADP release from the other[18,20,21]. Thus, the 'trapping' of the mobile neck linker concomitant with ATP binding by one head may enable ongoing conformational fluctuations in the partner head to become mechanically productive, thereby triggering ADP release and forward movement. As such, the two conformations of the kinesin neck linker in the disordered state[25] represent excellent candidates for the isomerization inferred from our mechanical studies.

Third, the model must describe the behaviour of kinesin as a function of load and ATP concentration. To test this prediction, we carried out a global analysis of kinesin-velocity data from three Michaelis–Menten curves at different loads and two curves of force against velocity at different ATP concentrations[5] (Fig. 2). The global fit using equations (1) and (4) successfully describes the single molecule velocity over three decades of ATP concentration and up to ~6 pN load. The model generates Michaelis–Menten parameters (Fig. 2a) that are statistically indistinguishable from those obtained previously by fitting to the individual curves[5]. The size of the fitted conformational change parameter, $\delta = 3.7 \pm 0.3$ nm, indicates that kinesin may make its 8-nm step along the microtubule in two ~4-nm stages.

The following picture emerges from fits to the model. Binding of ATP initiates a ~4-nm fluctuation between the two substates in rapid equilibrium. Forward rates from this rapid isomerization are greatly reduced by load. Immediately after exiting the composite state, a second, rapid advance of ~4 nm follows. This process is not rate-limiting at any load and is therefore not identical to the first substep. The model therefore makes a further prediction: displacement records of sufficiently high bandwidth should exhibit 4-nm

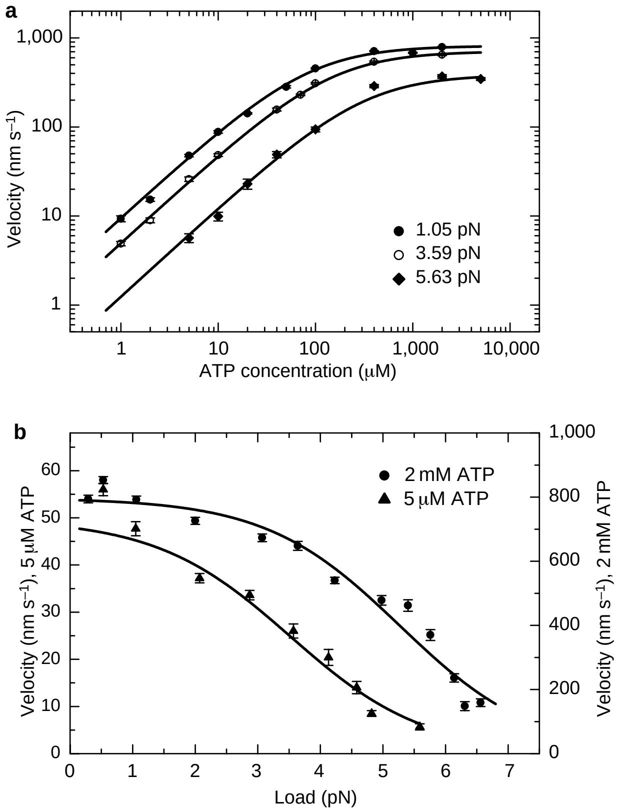

Figure 2 **Global fits of velocity to equations (1) and (4).** Solid lines represent fits to velocity data from ref. 5. There were 38 degrees of freedom and 5 independent parameters: $\delta = 3.7 \pm 0.3$ nm; $k^0_{cat} = 103 \pm 2\ s^{-1}$; $k^0_b = 1.3 \pm 0.1\ \mu M^{-1}\ s^{-1}$; $q_{cat} = 6.2 \pm 2.7 \times 10^{-3}$; $q_b = 4.0 \pm 1.4 \times 10^{-2}$. **a**, Double logarithmic plot of average bead velocity, v, against ATP concentration for various loads (filled circles, 1.05 ± 0.01 pN, n = 11–102 runs; open circles, 3.59 ± 0.03 pN, n = 8–79 runs; diamonds, 5.63 ± 0.06 pN, n = 19–58 runs). $V_{max} = 814 \pm 16\ nm\ s^{-1}$, $K_M = 85 \pm 4\ \mu M$, $F = 1.05 \pm 0.01$ pN; $V_{max} = 705 \pm 17\ nm\ s^{-1}$, $K_M = 142 \pm 7\ \mu M$, $F = 3.59 \pm 0.03$ pN; $V_{max} = 383 \pm 23\ nm\ s^{-1}$, $K_M = 310 \pm 43\ \mu M$, $F = 5.63 \pm 0.06$ pN. **b**, Average bead velocity, v, against applied load at fixed ATP concentrations (triangles, left axis, 5 μM ATP, n = 19–57 runs; circles, right axis, 2 mM ATP, n = 37–87 runs). Values are means ± s.e.m.

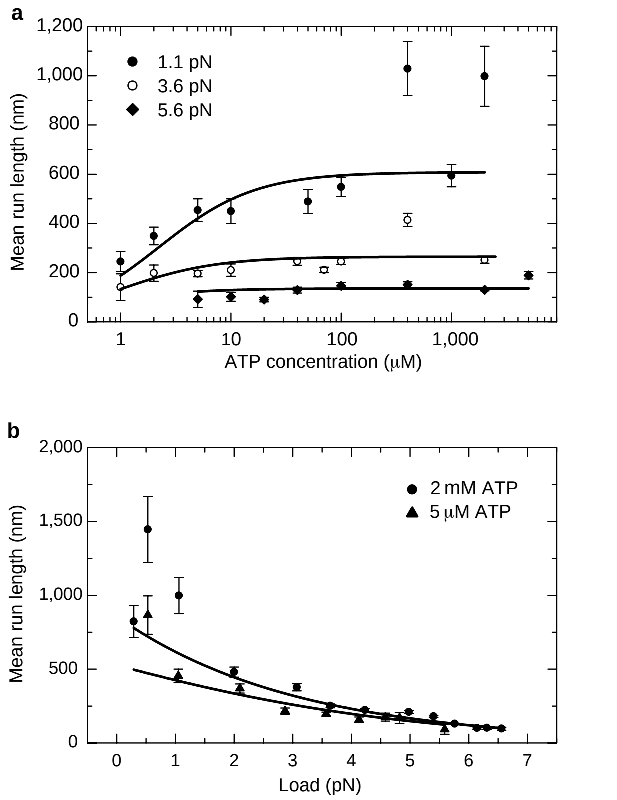

Figure 3 **Global fits of mean run length to equation (5).** Solid lines show fits. There were 37 degrees of freedom and 3 independent parameters: $A = 107 \pm 9$; $B = 0.029 \pm 0.009\ \mu M$; $\delta_L = 1.3 \pm 0.1$ nm. **a**, Semi-logarithmic plot of mean run length, L, against ATP concentration at fixed loads (filled circles, $1.05\ pN \pm 0.01$, n = 38–239 runs; open circles, 3.59 ± 0.03 pN, n = 8–326 runs; diamonds, 5.63 ± 0.03 pN, n = 12–143 runs. **b**, Mean run lengths, L, against applied load at fixed ATP concentrations (triangles, 5 μM ATP, n = 12–182 runs; circles, 2 mM ATP, n = 108–815 runs). Values are means ± s.e.m.

substeps. Recordings with responses of up to ~1 kHz have yet to reveal any significant substructure[5,6,9], although recent studies with improved bandwidths (~10 kHz) indicate that 4-nm steps may exist on a timescale of ~100 μs (ref. 31).

At extreme loads, beyond those exerted by the force clamp (≥6 pN), at least one factor not incorporated in equation (4) must reduce the velocity of kinesin. Experimental determinations of stall forces show that the maximum load-bearing capacity of the motor is ~5.5–7.5 pN, depending upon ATP concentration[5]. However, equations (1) and (4) lead to force–velocity curves with exponential tails at high loads (Fig. 2b), implying that forces as great as ~9–11 pN should be required to reduce speeds to insignificant levels. What additional factor reduces the velocity at extreme load? We can rule out a mechanism based on an increase in rearward stepping, because the small fraction of 8-nm steps directed backwards (~5–10%) does not increase substantially with load[5,6,8,9]. We are also inclined to discount the possibility an additional load-dependent transition that becomes rate-limiting at extreme loads: this would lead to a reduction in displacement fluctuations under such loads, whereas fluctuations are known to increase[5]. The possibility that we favour is that hydrolyses of ATP occur off the main kinetic pathway at extreme loads, and thereby fail to yield forward motion. Such futile turnovers would lead to a reduction in the ATP-coupling ratio and to a concomitant increase in displacement fluctuations[5]. Because displacement data indicate a negligible increase in the occurrence of 8-nm backwards steps under high loads[5], load does not reverse successful steps. Rather, the futile pathway must branch off the main pathway before the completion of the 8-nm step. To test this scenario, we modified the model by introducing load-dependent futile turnovers (see Methods). In the physiological regime (up to ~5 pN), fitted velocity and kinetic parameters were statistically indistinguishable from those of the previous description. The modified model reproduces strict 1:1 tight coupling at loads of up to ~5.5 pN, and predicts a rise in stall force with increasing ATP levels that matches published measurements[5] to within fractions of a pN (data not shown). These findings indicate that the ATPase cycle may uncouple from mechanical progress at extreme loads, but reinforce the validity of 1:1 tight coupling and the energy-landscape formalism in the physiological regime.

Kinesin processivity data and modelling. The energy-landscape picture may be used to model kinesin processivity. Using a single-molecule bead assay, we measured molecular run lengths over a range of loads and ATP concentrations (Fig. 3; see Methods). As shown previously[32,33], run lengths are exponentially distributed under fixed load and buffer conditions. When we varied the concentration of ATP at a given load, the mean run length, L, exhibited Michaelis–Menten behaviour, $L = L_0[\mathrm{ATP}]/([\mathrm{ATP}] + L_M)$, with a weakly load-dependent Michaelis constant, L_M. At low loads and

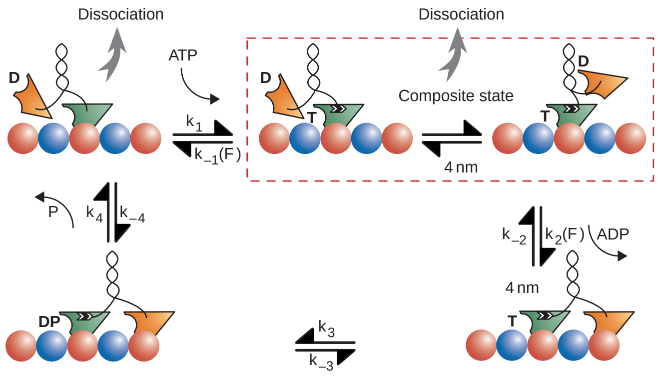

Figure 4 **Proposed mechanochemical cycle of kinesin.** The two kinesin heads (orange, green) are joined by their neck linker regions to a common coiled-coil stalk (black). T, ATP; D, ADP; P, inorganic phosphate. Strong binding occurs when a kinesin head makes contact with the microtubule protofilament (red, blue); other states correspond to weak or no binding. Initially, the forward head binds to the microtubule; the trailing head is free and binds to ADP. Upon binding of ATP to the forward head, kinesin enters a composite state (dashed red box), in which it undergoes rapid conformational fluctuations of ~4-nm along the microtubule. The forward rate of leaving this composite state, $k_2(F)$, and the backward rate, $k_{-1}(F)$, are both load-dependent. Binding of ATP also promotes the association of the neck linker region with the bound head[25] (black and white 'zipper' motif). Conformational fluctuations of the weakly bound head eventually allow binding to the next attachment site along the microtubule, triggering a further 4-nm advance and release of ADP. Both heads are now strongly bound. Subsequent hydrolysis and release of phosphate by the rearward head returns kinesin to the initial state, but translocated along the microtubule by 8-nm and with the heads interchanged. At extreme loads, futile hydrolysis can occur after binding of ATP but before completion of the 8-nm step, for example in the composite state. Kinesin can dissociate from the microtubule with small probability before ATP binding, but with higher probability after ATP binding. The latter, load-dependent, disassociation route may occur during rapid transitions within the composite state, while the motor has only one head attached to the microtubule (see text).

high ATP levels, L was ~600 nm, which is comparable to previous values[32,33]. L fell to ~300 nm when the ATP concentration was reduced to 5 μM, and to ~80 nm when load was increased to 5 pN. L declined approximately exponentially with load at a fixed ATP concentration (Fig. 3b). The characteristic distance parameter associated with this decline, $\delta_L = 1.3 \pm 0.1$ nm, is smaller than that for velocity, implying that the load-dependent events that are responsible for disassociation and for translocation are distinct.

What gives rise to the ATP-dependence of processivity? Our data enable us to rule out the simplest ATP-dependent mechanism, in which kinesin motors detach from the microtubule from state 1 (the state immediately before binding of ATP; equation (3)), as this would generate a mean run length that increases linearly with ATP concentration. A second mechanism, wherein detachment occurs from state N, leads to a Michaelis–Menten relationship but has two unattractive features. First, it requires the existence of another state, with only one motor head attached to the microtubule, in addition to those involved in translocation. Second, the transition from state N back to state 1 is generally thought to involve product release[17–21]. Thus, for disassociation to be measurably ATP-dependent, and also to occur from state N, there must be significant product rebinding. The probability of this was very low in our motility assays, as both ADP and phosphate concentrations were typically <10 nM. That said, state N in the kinesin cycle may have a shorter lifetime than intermediates so far identified by transient kinetic methods[17–21], and therefore may not involve product release after all. In any case, this scenario produces quantitative predictions that are almost indistinguishable from those of the next mechanism that we will consider.

A third mechanism, which we favour, allows detachment of the head to occur from either of two distinct states — state 1 and one other state that occurs after ATP binding. This can lead to a Michaelis constant that is small, L_M ~2 μM. A necessary condition is that the probability of detachment from state 1 is much lower than the probability of detachment from the second state, at least when ATP levels are greater than L_M. At high nucleotide levels, ATP binding occurs quickly, and therefore the probablility of disassociation from state 1 remains low. At lower ATP concentrations, however, the duration of state 1 increases, raising the probability of detachment from this state. To reproduce the exponential decline in L with load, the ATP-independent route for disassociation should exhibit load-dependent unbinding that is governed by Arrhenius–Eyring kinetics. The two routes for dissociation yield the following three-parameter expression for L:

$$L = \frac{8\ \text{nm}\cdot[\text{ATP}]\cdot Ae^{-F\delta_L/k_BT}}{[\text{ATP}] + B(1 + Ae^{-F\delta_L/k_BT})} \qquad (6)$$

where δ_L is the characteristic distance associated with load dependence. This leads to an almost exponential decline of L with load, with small corrections. Parameters A and B determine the likelihood of detachment through the load-dependent and ATP-dependent routes, respectively.

Run-length data obtained with the molecular force clamp (Fig. 3) are well described by equation (5), with $\delta_L = 1.3 \pm 0.1$ nm. Here, fitted parameter $A = 107 \pm 9$ gives the maximum average number of catalytic cycles before detachment, and is consistent with experimental values obtained in the absence of load[32,33]. The probability of detachment per cycle from state 1 is given by B/[ATP], where $B = 0.029 \pm 0.009$ μM. The Michaelis constant, $L_M = B(1 + Ae^{-F\delta_L/k_BT})$, declines slightly from 2.3 ± 0.8 μM at 1.05 pN to 1.0 ± 0.3 μM at 3.59 pN, and to 0.53 ± 0.2 μM at 5.63 pN. The energy-landscape formalism thus accounts for the effects of load and ATP levels on processivity as well as on velocity.

Discussion

Micromechanical measurements and modelling may be combined with recent biochemical[17–21,23,24] and structural[25] studies to provide a synthetic view of how kinesin motors may generate force in a tightly-coupled manner. Biochemical studies imply the existence of some form of mechanical signal that informs one kinesin head that ATP has bound to the other, thereby triggering ADP release from the former in the presence of a microtubule. Structural studies have shown that, in the absence of ATP, the neck linker region exists in multiple configurations, and that binding of ATP serves to stabilize this domain, causing it to associate more tightly with the motor core. Here we have provided evidence that a rapid, load-dependent isomerization following ATP binding is critical for motility and can quantitatively account for micromechanical data.

The following picture of the kinesin cycle emerges (Fig. 4): ATP binding triggers the first of two rapid 4-nm components that make up the overall 8-nm step, causing the neck linker of the microtubule-bound head of the kinesin dimer to become immobilized and bind to its motor core. Fluctuating interactions between the neck linker and motor domain of the free head induce transient 4-nm movements that are directed productively along the microtubule. As the bound and unbound conformations of the mobile neck linker are separated by only ~1–2 k_BT of energy at negligible loads (S. Rice and R. Cooke, personal communication), these 4-nm fluctuations are likely to occur on timescales that are shorter than 1 ms. Eventually, one of these fluctuations permits the free kinesin head to reach and bind to the next microtubule-attachment site, inducing a further 4-nm advance along with rapid ADP release. Release of ADP, which has been found to be slow for unloaded single-headed kinesin molecules[34], is expected to be activated by load and so probably occurs either at the same time as or immediately after the second 4-nm step.

Thus, the energy of hydrolysis is not used to drive an immediate, large conformational change, as in the classic swinging-cross-bridge mechanism for myosin[22] and in a recently proposed mechanism for kinesin[35]. Instead, energy from hydrolysis might be stored in the enzyme, perhaps in the form of an internal strain. The two conformational changes follow only upon ATP binding to the opposite head; this ensures tight 1:1 coupling, because the energy from one ATP hydrolysis is apparently used to prevent the next ATP molecule from hydrolysing until an 8-nm step has been completed. However, at extreme loads, a futile hydrolysis may occur after ATP binding but before completion of the 8-nm step, for example in state 2 of Fig. 4. A small fraction of disassociation events from the microtubule occur while awaiting the arrival of the next ATP molecule, but the majority of disassociations occur after ATP binding, during transitions in which only one head is attached to the microtubule (Fig. 4). Because processivity and velocity have different functional dependencies on load ($\delta_L = 1.3 \pm 0.1$ nm compared with $\delta = 3.7 \pm 0.3$ nm), it seems likely that distinct, load-dependent events govern their respective behaviors. Load-dependent disassociation may occur from the composite state 2, possibly during transitions between the substates in which the motor has only one head attached to the microtubule.

The composite-state mechanism of kinesin motility gives rise to several more testable predictions. In the model, load reduces the affinity of ATP by increasing the unbinding rate rather than by lowering the binding rate. Furthermore, the time between binding of ATP to one head and release of ADP from the other head increases with load, as the equilibrium shifts to the rearward conformation of the composite state (state 2). However, once the ADP-bearing head binds to the microtubule, release of ADP should be activated by load. This might be explored using single-motor assays that combine fluorescence and optical tweezers, and quantified using single-headed kinesin in conjunction with a three-bead geometry similar to that used to study individual myosin motors[36]. A key prediction is that the rate of mechanical transitions between the two isomerization substates should be load-dependent, but independent of ATP concentration. The ratio of the transition rates between the two substates will be $K = K_0 e^{-F\delta/k_BT}$.

The kinetics of kinesin may be optimized, in certain respects, to support its function as an efficient cellular transporter. *In vivo*, the distribution of loads experienced by motors carrying vesicles along microtubules is expected to be bimodal; under typical circumstances, a vesicle is freely tethered to its motor, and the viscous drag force associated with pulling it through the cytosol remains low. However, when the vesicle occasionally snags on a cytoskeletal element, such as an actin fibre, intermediate filament or microtubule, the load increases markedly. The mechanochemistry and processivity of kinesin seem to be tuned in such a way that motors maintain tight coupling for all reasonable loads that support continuous movement. However, when faced with an insuperable obstacle, a motor will become detached to avoid spending much time in a mode in which it is forced to undergo cycles of futile ATP hydrolysis. This strategy enables vesicles powered by single motors (or just a few motors) to release and diffuse away from barriers briefly, then to rebind to the microtubule skeleton and resume forward progress without wasting energy.

The ability of the free-energy-landscape formalism to account for mechanical observations in both the kinesin and RNAP systems indicates that it may supply a general framework for understanding a wide range of mechanoenzymes. Unidirectional motors such as polymerases, helicases and nucleases may well fall within this category. Although the unique structural characteristics of each of these enzymes suggest different microscopic mechanisms of motility, energetic considerations, such as those presented here, may nevertheless provide a unified view of how motors work. □

Methods

Motility assays.

Motility assays were carried out as described[3,5]. Briefly, glass beads (0.5-µm diameter) coated with single kinesin molecules were optically trapped and placed onto microtubules attached to a glass coverslip. Subsequent measurements of velocity and processivity were made using a molecular force clamp[5,37], which maintains a constant load on a kinesin molecule by maintaining a fixed distance between the optical trap and the bead; the position of the bead was measured using a quadrant photodiode[38]. Displacement records obtained within ±150 nm of the centre of the detector were used for analysis.

Analysis.

Global fits of velocities and mean run lengths to theoretical models were achieved by non-linear optimization using custom software written in MatLab 5.0 (MathWorks). Experimentally determined values and fitted model parameters are expressed as means ± s.e.m. Distances were measured directly for runs of length $R < 300$ nm that terminated inside the detector region. We confirmed that run lengths of <300 nm were exponentially distributed at high loads (data not shown). The mean run length (L) of all runs, including those longer than R that were not measured directly with our instrument, was calculated in two stages. First, for each ATP level and load, the average length, $\tilde{L}$, and the fraction of runs that terminated inside the detector region, f, were determined. Next, L was calculated using $L = \tilde{L} + R(1-f)/f$, which was derived by assuming an exponential parent distribution. To investigate the possibility that load-dependent futile hydrolysis occurred at extreme loads (>5.5 pN), velocity fits were repeated with a load-dependent efficiency factor $\varepsilon(F) = 1/(1 + \kappa \exp(F\delta_N/k_BT))$ incorporated into the numerator of equation (1), where $\kappa << 1$ and δ_N fix the unloaded probability and load dependence of futile hydrolysis, respectively.

RECEIVED 1 JUNE 2000; REVISED 19 JUNE 2000; ACCEPTED 3 JULY 2000;
PUBLISHED 14 SEPTEMBER 2000.

1. Howard, J. Molecular motors: structural adaptations to cellular functions. *Nature* **389**, 561–567 (1997).
2. Svoboda, K., Schmidt, C. F., Schnapp, B. J. & Block, S. M. Direct observation of kinesin stepping by optical trapping interferometry. *Nature* **365**, 721–727 (1993).
3. Schnitzer, M. J. & Block, S. M. Kinesin hydrolyses one ATP per 8-nm step. *Nature* **388**, 386–390 (1997).
4. Howard, J., Hudspeth, A. J. & Vale, R. D. Movement of microtubules by single kinesin molecules. *Nature* **342**, 154–158 (1989).
5. Visscher, K., Schnitzer, M. J. & Block, S. M. Single kinesin molecules studied with a molecular force clamp. *Nature* **400**, 184–189 (1999).
6. Svoboda, K. & Block, S. M. Force and velocity measured for single kinesin molecules. *Cell* **77**, 773–784 (1994).
7. Meyhöfer, E. & Howard, J. The force generated by a single kinesin molecule against an elastic load. *Proc. Natl Acad. Sci. USA* **92**, 574–578 (1995).
8. Coppin, C. M., Pierce, D. W., Hsu, L. & Vale, R. D. The load dependence of kinesin's mechanical cycle. *Proc. Natl Acad. Sci. USA* **94**, 8539–8544 (1997).
9. Kojima, H., Muto, E., Higuchi, H. & Yanagida, T. Mechanics of single kinesin molecules measured by optical trapping nanometry. *Biophys. J.* **73**, 2012–2022 (1997).
10. Peskin, C. & Oster, G. Coordinated hydrolysis explains the mechanical behavior of kinesin. *Biophys. J.* **68**, 202s–211s (1995).
11. Duke, T. & Leibler, S. Motor protein mechanics: a stochastic model with minimal mechanochemical coupling. *Biophys. J.* **71**, 1235–1247 (1996).
12. Derényi, I. & Vicsek, T. The kinesin walk: a dynamic model with elastically coupled heads. *Proc. Natl Acad. Sci. USA* **93**, 6775–6779 (1996).
13. Astumian, R. D. Thermodynamics and kinetics of a brownian motor. *Science* **276**, 917–922 (1997).
14. Howard, J. The mechanics of force generation by kinesin. *Biophys. J.* **68**, 245s–255s (1995).
15. Wang, M. D. *et al.* Force and velocity measured for single molecules of RNA polymerase. *Science* **282**, 902–907 (1998).
16. Hille, B. *Ionic Channels of Excitable Membranes* (Sinauer Associates, Sunderland, Massachusetts, 1992).
17. Ma, Y. Z. & Taylor, E. W. Mechanism of microtubule kinesin ATPase. *Biochemistry* **34**, 13242–13251 (1995).
18. Ma, Y. Z. & Taylor, E. W. Interacting head mechanism of microtubule-kinesin ATPase. *J. Biol. Chem.* **272**, 724–730 (1997).
19. Gilbert, S. P., Webb, M. R., Brune, M. & Johnson, K. A. Pathway of processive ATP hydrolysis by kinesin. *Nature* **373**, 671–676 (1995).
20. Gilbert, S. P., Moyer, M. L. & Johnson, K. A. Alternating site mechanism of the kinesin ATPase. *Biochemistry* **37**, 792–799 (1998).
21. Moyer, M. L., Gilbert, S. P. & Johnson, K. A. Pathway of ATP hydrolysis by monomeric and dimeric kinesin. *Biochemistry* **37**, 800–813 (1998).
22. Bagshaw, C. R. *Muscle Contraction.* (Chapman and Hall, London, 1993).
23. Hackney, D. D. Evidence for alternating head catalysis by kinesin during microtubule-stimulated ATP hydrolysis. *Proc. Natl Acad. Sci. USA* **91**, 6865–6869 (1994).
24. Hackney, D. D. Highly processive microtubule-stimulated ATP hydrolysis by dimeric kinesin head domains. *Nature* **377**, 448–450 (1995).
25. Rice, S. *et al.* A structural change in the kinesin motor protein that drives motility. *Nature* **402**, 778–784 (1999).
26. Hua, W., Young, E. C., Fleming, M. L. & Gelles, J. Coupling of kinesin steps to ATP hydrolysis. *Nature* **388**, 390–393 (1997).
27. Case, R. B., Rice, S., Hart, C. L., Ly, B. & Vale R. D. Role of the kinesin neck linker and catalytic core

in microtubule-based motility. *Curr. Biol.* **10,** 157–160 (2000).
28. Case, R. B., Pierce, D. W., Hom-Booher, N., Hart, C. L. & Vale, R. D. The directional preference of kinesin motors is specified by an element outside of the motor catalytic domain. *Cell* **90,** 959–966 (1997).
29. Henningsen, U. & Schliwa, M. Reversal in the direction of movement of a molecular motor. *Nature* **389,** 93–96 (1997).
30. Endow, S. A. & Waligora, K. W. Determinants of kinesin motor polarity. *Science* **281,** 1200–1202 (1998).
31. Nishiyama, M. *et al.* The rising phase of kinesin's 8nm step. *Biophys. J.* **78,** 122A (2000).
32. Block, S. M., Goldstein, L. S. B. & Schnapp, B. J. Bead movement by single kinesin molecules studied with an optical tweezers. *Nature* **348,** 348–352 (1990).
33. Vale, R. D. *et al.* Direct observation of single kinesin molecules moving along microtubules. *Nature* **380,** 451–453 (1996).
34. Hancock, W. O. & Howard, J. Kinesin's processivity results from mechanical and chemical coordination between the ATP hydrolysis cycles of the two motor domains. *Proc. Natl Acad. Sci. USA* **96,** 13147–13152 (1999).
35. Cross, R. A., Crevel, I., Carter, N. J., Alonso, M. C., Hirose, K. & Amos, L. A. The conformational cycle of kinesin. *Phil. Trans. R. Soc. Lond. B* **355,** 459–464 (2000).
36. Finer, J. T., Simmons, R. M. & Spudich J. A. Single myosin molecule mechanics: piconewton forces and nanometre steps. *Nature* **368,** 113–119 (1994).
37. Visscher, K. & Block, S. M. Versatile optical traps with feedback control. *Methods Enzymol.* **298,** 460–489 (1998).
38. Visscher, K., Gross, S. P. & Block S. M. Construction of multiple-beam optical traps with nanometer-resolution position sensing. *IEEE J. Sel. Topics Quant. Elect.* **2,** 1066–1076 (1996).

ACKNOWLEDGEMENTS
We thank T. Perkins and L. Satterwhite for helpful discussions, J. de Georgis for squid dissection, and D. Peoples for expert machining. Experiments were carried out at Princeton University and were supported by grants from the NIGMS, NSF and W.M. Keck Foundation (to S.M.B.), predoctoral fellowships from the American Heart Association, the Charlotte Elizabeth Proctor Fund and the Program in Mathematics and Molecular Biology Burroughs Wellcome Fund (to M.J.S.), and a postdoctoral fellowship from the Burroughs Wellcome Fund of the Life Sciences Research Foundation (to K.V.). Data analysis and modelling were also supported by Lucent Technologies.
Correspondence and requests for materials should be addressed to K.V. or S.M.B.